Comparison of proto-oncogenic and mutant forms of the transmembrane region of the Neu receptor in TFE

R. Scott Houliston[a], Robert S. Hodges[b], Frances J. Sharom[a], James H. Davis[c,*]

[a] *Department of Chemistry and Biochemistry, University of Guelph, Guelph, ON, Canada N1G 2W1*
[b] *Department of Biochemistry and Molecular Genetics, University of Colorado Health Sciences Centre, Denver, CO 80262, USA*
[c] *Department of Physics, University of Guelph, Guelph, ON, Canada N1G 2W1*

Received 11 September 2002; revised 19 November 2002; accepted 19 November 2002

First published online 24 December 2002

Edited by Thomas L. James

Abstract A single mutation within the transmembrane region of the Neu receptor ($Val^{664} \rightarrow Glu$) is known to enhance tyrosine kinase activity, by promoting receptor dimerization. In order to gain insight into potential structural changes that arise as a result of the mutation, peptides corresponding to the complete transmembrane domain of proto-oncogenic and mutant forms of Neu have been studied by ^1H nuclear magnetic resonance in the solvent trifluoroethanol (TFE). The chemical shifts are similar for both forms of the peptide, with the exception of amide residues close to the mutation site. Both peptides adopt a helical conformation, with a distinct bend one turn downstream of the mutation site. This deformation gives rise to several nuclear Overhauser effects, the majority of which were detected in both peptides, that are atypical for a straight canonical α-helix. Our data in this solvent do not support a conformational change in the transmembrane domain of monomeric Neu as a result of the mutation. Sodium dodecyl sulfate–polyacrylamide gel electrophoresis analysis indicates that proto-oncogenic Neu peptides have a higher propensity to oligomerize in the solvent TFE than the Glu^{664} oncogenic form.

Key words: Neu/ErbB-2; Receptor tyrosine kinase; Transmembrane domain; Nuclear magnetic resonance structure; Trifluoroethanol

1. Introduction

The catalytic activation of many receptor tyrosine kinases (RTKs) occurs following dimerization, leading to the phosphorylation of intracellular substrates [1,2]. RTKs initiate growth and differentiation pathways, and their level of activity is predominantly influenced by the binding of cognate growth factors. In some instances however, a mutation within the transmembrane domain of these receptors promotes dimerization, and subsequent kinase activity in the absence of ligand binding [3–6].

One example of modulated activity resulting from a mutation in the transmembrane domain of a tyrosine kinase receptor occurs in Neu/ErbB-2, a member of the epidermal growth factor receptor (EGFR) subfamily. The replacement of a valine residue at position 664 of Neu with glutamic acid has been shown to increase receptor dimerization and kinase activity [7–9], and leads to a transforming phenotype in some cell lines [10].

As yet, there is no indisputable formulation to explain the physical basis for enhanced receptor dimerization and activity upon mutation. One theory provides that enhanced receptor interaction occurs as a result of inter-receptor hydrogen bonding involving the side chain carboxyl group of glutamic acid [11]. This has been postulated to occur via symmetrical bidentate hydrogen bonds between the glutamate side chains of adjacent receptors [12], or alternatively, between the side chain of one receptor and the amide backbone of another [13,14]. Another theory, not incompatible with the former, favors a structural reorientation of the transmembrane domain upon mutation, that facilitates inter-helical dimeric interactions. Wide-line ^2H nuclear magnetic resonance (NMR) spectral differences between monomeric forms of proto-oncogenic and mutant Neu/ErbB-2 peptides in bilayers have been observed, and are largely dependent on the position of the ^2H probe within the transmembrane region [15,16]. Probes upstream of the mutation site exhibited similar splitting patterns, while the probes close to and downstream of the mutation site had noticeably different quadrupolar splitting. These results were ascribed to limited structural differences between the two forms of the peptide.

Results of theoretical studies on the Neu/ErbB-2 transmembrane domain have illuminated potential structural changes that might arise due to the transforming mutation. Using conformational energy analysis, Brandt-Rauf et al. [17,18] have predicted that the favored conformation of the proto-oncogenic receptor would exhibit a sharp bend at the mutation site, whereas a straight α-helical conformation would be favored for the mutant. In a separate study, π-bulge distortions due to backbone hydrogen bond rearrangements were observed in molecular dynamics (MD) simulations of the ErbB-2 transmembrane domain performed in vacuo [19], and might be favored in proto-oncogenic peptides over mutated ones.

There have been two reported studies on the structure of peptides corresponding to the transmembrane domain of Neu

*Corresponding author. Fax: (1)-519-836 9967.
E-mail address: jhd@physics.uoguelph.ca (J.H. Davis).

Abbreviations: TFE, trifluoroethanol; RTK, receptor tyrosine kinase; ErbB-2, protein product of HER2 (or c-erbB-2), a class I tyrosine kinase receptor; Neu, rat analogue of ErbB-2; EGFR, epidermal growth factor receptor; MD, molecular dynamics; NOESY, nuclear Overhauser effect spectroscopy; TOCSY, total correlation spectroscopy; SDS–PAGE, sodium dodecyl sulfate–polyacrylamide gel electrophoresis; r.m.s., root mean square

0014-5793/02/$22.00
doi:10.1016/S0014-5793(02)03852-8

in the solvent trifluoroethanol (TFE). Gullick et al. [20] synthesized 18 residue peptides representing a portion of the transmembrane region, with some hydrophobic residues replaced with serine. Both peptides adopted a straight canonical helical structure, and there was no discernible conformational change observed between proto-oncogenic and mutant forms of the peptides. The structure of a 35 residue peptide corresponding to the entire transmembrane domain of proto-oncogenic Neu has been reported by Goetz et al. [21]. They reported a seven residue π-bulge distortion, downstream of the mutation site, centered around four consecutive valine residues (Val^{673}–Val^{676}). This distortion was similar to that seen in MD simulations [19,22]. In this study, no results were reported for the mutant form of the transmembrane domain.

We have initiated NMR studies on transmembrane Neu peptides, in order to establish potential structural and/or dynamic changes that arise as a result of the transforming mutation. In this investigation, we report NMR-derived structures in TFE, for two chemically synthesized peptides that incorporate the putative transmembrane domain of both proto-oncogenic and mutant receptors. The proton chemical shifts and nuclear Overhauser effect (NOE) connectivities for both molecules are similar, and consistent with an α-helical structure. We detected a flexible region in the two peptides, which gave rise to a distinct bend in the conformation roughly one helical turn downstream of the mutation site. To assess their level of aggregation following TFE exposure, the peptides were analyzed using sodium dodecyl sulfate–polyacrylamide gel electrophoresis (SDS–PAGE), which indicates that proto-oncogenic Neu peptides form higher order aggregates more readily in this solvent than the mutant peptides.

2. Materials and methods

2.1. Peptide synthesis

Peptides of 36 amino acids, comprising residues adjacent to and including the putative transmembrane domain of proto-oncogenic and mutant Neu, were synthesized using the FMOC strategy, and purified by reversed-phase chromatography. The purity of the peptides was confirmed by mass spectrometry.

The sequence of the proto-oncogenic peptide, corresponding to the position of the amino acids within the Neu receptor, is: Q^{651}RASPVTFIIATVV^{664}GVLLFLILVVVVGILIKRRRQK^{686}. The mutant peptide has an identical sequence, except at position 664, where valine is replaced with glutamic acid. Within our peptides the mutation site corresponds to residue 14.

2.2. NMR spectroscopy and structure determination

Approximately 1.5 mg of purified peptide was dissolved in 0.5 ml of d_2-TFE (Cambridge Isotope Laboratories), to give a concentration of ~1.5 mM. 2D-Homonuclear correlation spectra were acquired at 303 K, on a Bruker Avance spectrometer operating at 600 MHz, with a spectral window of 10.1 ppm. Chemical shifts were referenced with respect to the residual methylene protons of TFE, appearing at 3.88 ppm. NOESY spectra, with mixing times of 150, 200 and 300 ms, were acquired using a presaturation pulse during the relaxation delay to suppress the OH resonance of TFE, and using time-proportional phase increment for quadrature detection. Scalar coupled networks were assigned with total correlation spectroscopy (TOCSY) spectra acquired using a decoupling in the presence of scalar interactions (DIPSI)-2 [23] pulse scheme, isotropic mixing times of 30, 60, and 75 ms, solvent suppression using WATERGATE [24], and an echo–antiecho phase cycle for quadrature detection. All 2D spectra were acquired with 2048 data points in the direct dimension, 256 points in the indirect dimension, and 256 scans per increment.

NMR data were processed using the software Felix97 (Biosym), on an O2 workstation (Silicon Graphics). Shifted sine-bell (90°) window functions were applied to the transients prior to Fourier transformation. The final matrix size was 2048×512, corresponding to a digital resolution of 2.9 Hz/point in the direct dimension, and 11.7 Hz/point in the indirect dimension.

NOE distance restraints were obtained from integrated cross-peaks obtained from NOESY spectra with mixing times of 300 ms. Based on peak volumes, NOEs were classified as either 'strong', 'medium', or 'weak', corresponding to restraint distances of <3.5, <4.5, and <6.0 Å respectively. In all cases, a lower bound distance restraint of 2.0 Å was applied. Correction factors for pseudoatoms were added to these limits as described by Wüthrich et al. [25]. The calculation of energy-minimized structures was carried out using the program X-PLOR [26]. One hundred embedded substructures were generated and regularized by simulated annealing [27], with an initial temperature of 3000 K, using 2000 high temperature cycles of restrained energy minimization followed by 3 ps restrained molecular Verlet dynamics. Two thousand cooling steps were performed to a final temperature of 300 K. During cooling, the van der Waals interactions were increased by varying the van der Waals repel function from 0.003 to 4 kcal/mol/Å^4. Structures obtained from simulated annealing were further refined [28] through 10 000 cycles of restrained energy minimization. A square-well restraining function was used for the effective NOE energy term. During all calculations, side chain groups were uncharged. Twenty-two structures with the lowest energy and without NOE violations >0.1 Å were chosen for further analysis.

2.3. Gel electrophoresis

Peptides were dissolved in standard loading buffer [29], incubated at 42°C for 30 min, and run on a 16.5% Tris-tricine gel [30]. The gel was stained with Coomassie brilliant blue. Peptides pretreated with TFE were incubated for 1 h at room temperature, and the TFE was evaporated under a steady stream of N_2.

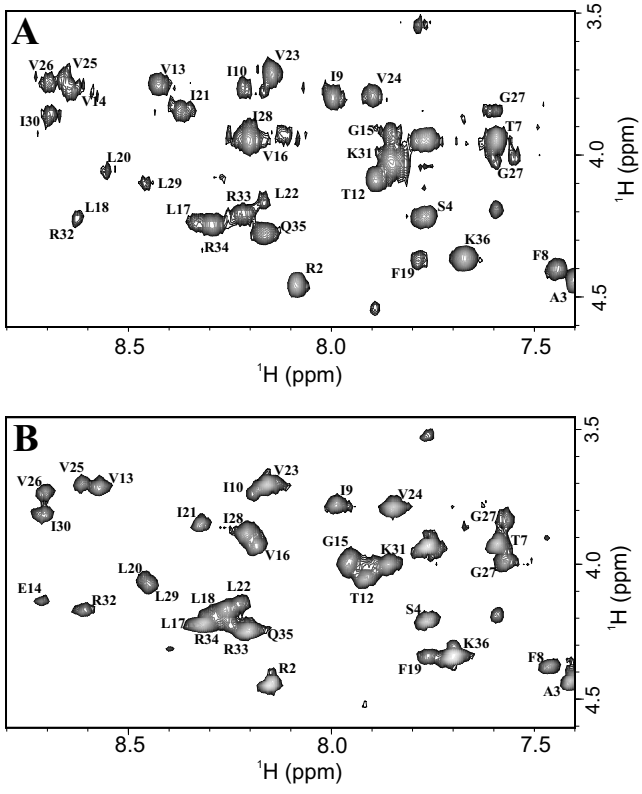

Fig. 1. TOCSY spectra corresponding to the NH–CHα region of Neu peptides. Spectra are of (A) proto-oncogenic and (B) mutant peptide in TFE at 30°C, with the NH-CHα cross-peaks labeled. Some of the amide proton chemical shifts differ between the two peptides for residues within 1.5 helical turns of mutation site, whereas the CHα chemical shift does not change significantly for any residue.

3. Results

Standard homonuclear correlation experiments were used to assign the resonances of both proto-oncogenic and mutant Neu peptides, and to obtain restraint distances for the calculation of their average structure in TFE. All of the NMR experiments were performed at peptide concentrations of 1.5 mM. Circular dichroism experiments on proto-oncogenic Neu peptides in this solvent [21] have indicated that there is minimal dimerization at concentrations less than 2 mM. The NH–CHα region of a TOCSY spectrum of both peptides is presented in Fig. 1. The majority of the cross-peaks for both peptides appear at the same chemical shift, with the exception of amide resonances within 1.5 helical turns of the mutation site. There is very little difference in the CHα chemical shifts for both peptides, and they are upfield of random coil values, indicating the residues are participants in an α-helix [31].

As indicated in Fig. 2, the NOE connectivity pattern for both peptides is typical of an α-helix, with several strong $H\alpha_i$–$H\beta_{i+3}$ and $H\alpha_i$–NH_{i+3} contacts for residues between 5 and 32. The pattern observed for each peptide is not identical. This is due in part to the movement of some amide resonances in the spectra, which caused the overlap of resonances in some regions of the NOESY spectra for one peptide, and not the other. This resulted in a slightly different complement of unambiguous NOE assignments for the two peptides. Also, residues at the C-terminus of the proto-oncogenic peptide yielded fewer NOEs than the analogous portion of the mutant peptide. Therefore, there was slightly poorer precision in the average structure derived for the proto-oncogenic peptide (as indicated by the root mean square (r.m.s.) values in Table 1).

Several NOEs, depicted in the lower portion of Fig. 2 (NH_i–NH_{i+4}, αH_i–βH_{i+4}, NH_i–αH_{i+5}), are indicative of a deviation from a straight canonical α-helix. Most were detected in both peptides, and appear roughly one helical turn downstream of the mutation site. These NOEs are indicative of a helical deformation, and give rise to a bend in the conformation of both peptides.

A total of 336 experimental distance restraints were used to deduce the conformation of the proto-oncogenic peptide, and 368 were used for the mutant peptide (Table 1). These calculations were performed using the program X-PLOR [26]. From an initial pool of 100 structures generated through simulated annealing, a family of 22 was selected for the calculation of the average conformation of each peptide. These structures had the lowest overall energy, and no NOE violations

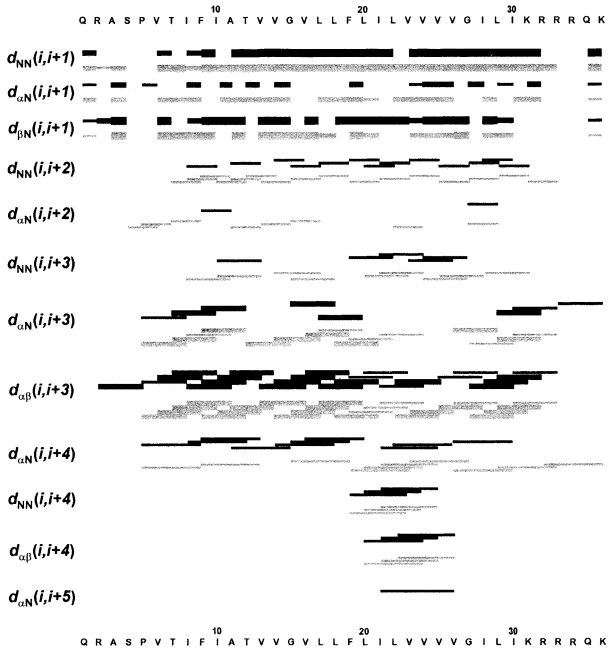

Fig. 2. NOE connectivities for Neu peptides. NOEs are shown as a function of the amino acid sequence for the proto-oncogenic (black lines) and mutant (gray lines) peptides, with the intensity of the NOE reflected by the line thickness.

greater than 0.1 Å. The superposition of the structures (Fig. 3) displays good precision, with r.m.s. deviations for backbone atoms of 1.38 and 1.25 Å for the proto-oncogenic and mutant peptides respectively. The final conformation of each peptide, shown in Fig. 3, was calculated based on the atoms of residues 5–32 averaged over the 22 structures in the family.

NMR experiments were performed at concentrations where peptide aggregation is believed to be minimal. Using SDS–PAGE, we also monitored whether there was evidence of aggregation upon exposure to TFE, followed by solvent evaporation – since studies in bilayers with peptides of this nature often involve solubilization in TFE before reconstitution. The peptides were exposed to either an H_2O/acetonitrile mixture containing 0.1% trifluoroacetic acid, where they are unfolded, or TFE, prior to incubation in standard SDS loading buffer. The interpretation of the migration pattern of transmembrane α-helices on polyacrylamide gels is complicated by the observation that these peptides tend to migrate at rates faster than

Table 1
Structural statistics for proto-oncogenic and mutant Neu peptides

	Proto-oncogenic	Mutant
Total experimental restraints	336	368
Intraresidual	133	134
Sequential	203	234
Number of structures used to determine average	22	22
Number of structures with restraint violations >0.1 Å	0	0
r.m.s. deviations (Å) to the average structure from residues 5–32:		
backbone atoms (N, C_α, C^a)	1.38	1.25
heavy atoms	1.89	1.76
all atoms	1.96	1.87
Ramachandran plot statistics for residues 5–32:		
Number of residues in most favored regions	27	26
Number of residues in additional allowed regions	3	3
Number of residues in generously allowed regions	0	1
Number of residues in disallowed regions	0	0

would be expected for a protein/peptide of similar mass [32]. Nonetheless, our results clearly demonstrate a differing migration pattern for the two peptides both before and after treatment with TFE, based on the extent of oligomerization (Fig. 4). Proto-oncogenic peptide, unfolded prior to incubation in the SDS buffer, runs as a single band on the gel, at roughly 1.5× its mass. Following TFE treatment, the peptide runs as a diffuse band containing higher order aggregates. The mutant peptide migrates predominantly at 1.0× its mass before and after TFE treatment, with a faint band appearing at 2.0× its mass.

4. Discussion

Elucidating the details of structural changes resulting from a point mutation in the Neu/ErbB-2 receptor may provide important insight into the activation mechanism of RTKs. Towards this end, several theoretical and experimental investigations on the transmembrane region of this receptor have been reported.

Smith et al. [12] determined that the glutamate side chains of mutant Neu oligomers reconstituted in bilayers were protonated and participants in a hydrogen bond, which could potentially stabilize dimeric interactions between receptors. ^{2}H NMR spectral differences have been observed between proto-oncogenic and mutant forms of Neu/ErbB-2 receptors in bilayers, and have been attributed to structural differences close to and downstream of the mutation site [15,16]. Conformational energy analysis predicted a bend in proto-oncogenic Neu peptides at the mutation site, which would hinder side-to-side association of the transmembrane domain – as opposed to the straight helical structure predicted for the mutant form [17,18]. MD simulations performed on ErbB-2 peptides in vacuo have exhibited π-bulge distortions [19,22]. π-bulges, also referred to as 'α aneurisms', have been observed experimentally in helices of several globular proteins [33–35]. A transition from an α- to a π-helix could alter the relative orientation of side chains of a helical face, which in turn could significantly impact the side-to-side interaction of adjacent helices.

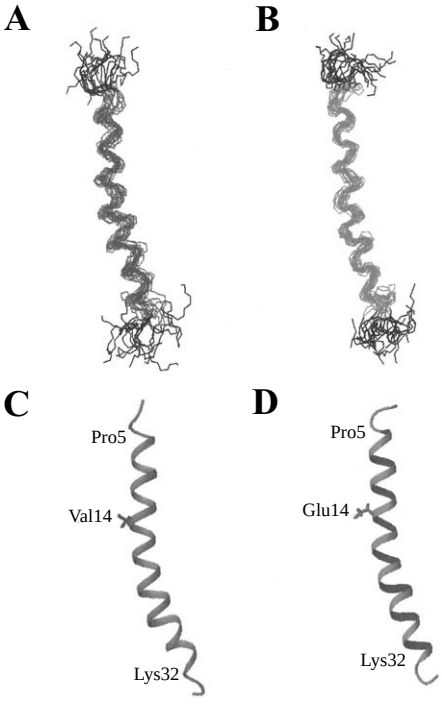

Fig. 3. Solution structure of Neu peptides in TFE. Displayed are the families of 22 structures for the (A) proto-oncogenic and (B) mutant forms of the peptide selected for the computation of the average conformation. These structures had no NOE violations greater than 0.1 Å, and had the lowest energy among those generated by simulated annealing. The ribbon representations of the (C) proto-oncogenic and (D) mutant Neu peptides are based on atoms in residues 5–32, averaged over the 22 structures. The figure was produced using the program MOLMOL [38].

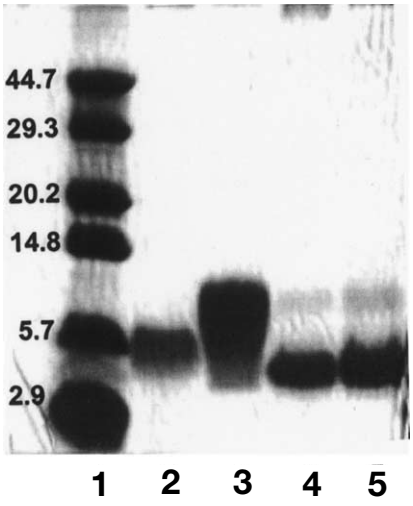

Fig. 4. SDS–PAGE analysis of Neu peptides. The lanes of the gel contain the proto-oncogenic form prior to (2) and following TFE treatment (3), and the mutant form prior to (4) and following TFE treatment (5). Standard molecular weight markers are in lane 1 labeled with their corresponding molecular mass (kDa). Monomeric forms of both Neu peptides have a molecular mass of ~4 kDa.

Based on our studies of Neu peptides in TFE, the conformation of the transmembrane domain of this receptor does not change as a result of the transforming mutation. This is supported by the agreement between the proton chemical shifts in both peptides, and by the similarity in their structures. Careful inspection of our spectra did reveal several NOEs that were indicative of a deviation from a straight helical conformation. Our resulting structures exhibited a distinct bend one turn downstream of the mutation site. The structure of a 35 residue proto-oncogenic Neu peptide in TFE was reported to contain a π-bulge downstream of the mutation site, spanning residues Ile^{671} to Gly^{677} [21], however no results were reported for the mutant form of the receptor. It is unclear why we did not see a π-bulge distortion in the proto-oncogenic form of the peptide. Goetz et al. [21] noted two NOEs that were indicative of a deviation from a standard canonical α-helix, specifically two NH_i–αH_{i+5} NOEs. We observed one NH_i–αH_{i+5} NOE (Ile^{671} to Val^{676}) in the proto-oncogenic form of the peptide. No NH_i–αH_{i+5} NOEs could be confirmed in the mutant form of the peptide. The methods used to calculate the structures differed as well; we used X-PLOR, which makes use of CHARMM force fields, whereas Goetz et al. used DYANA [36], which employs AMBER force fields.

A recent investigation using *Escherichia coli* cell membranes quantified the dimerization of constructs containing transmembrane domains from members of the EGFR family,

and demonstrated that, in contrast with other studies of full length receptors, constructs containing the proto-oncogenic form of the ErbB-2 transmembrane domain oligomerized more readily than those containing the mutant form [37]. SDS–PAGE analysis of our chemically synthesized Neu transmembrane peptides indicates that the proto-oncogenic form aggregates more readily than the mutant form upon exposure to TFE. Clearly, the extent to which these peptides will oligomerize under various conditions cannot be predicted based on studies with full length receptors. The propensity of these molecules to dimerize may be dictated by elements in the extra- and intracellular domains in addition to the transmembrane region.

Acknowledgements: We would like to thank Valerie Robertson, manager of the Guelph Food and Soft Materials Centre, for her guidance with the NMR experiments, and Marc Genest at the Canadian Protein Engineering Network (PENCE) for help in synthesizing the peptides. This work was supported by grants from the National Sciences and Engineering Council of Canada (NSERC), and by the Canada Foundation for Innovation (CFI).

References

[1] Lemmon, M.A. and Schlessinger, J. (1994) Trends Biochem. Sci. 19, 459–463.
[2] Schlessinger, J. (1988) Trends Biochem. Sci. 13, 443–447.
[3] Jenkins, B.J., D'Andrea, R. and Gonda, T.J. (1995) EMBO J. 14, 4276–4287.
[4] Longo, N., Shuster, R.C., Griffin, L.D., Langley, S.D. and Elsas, L.J. (1992) J. Biol. Chem. 267, 12416–12419.
[5] Miloso, M., Mazzotti, M., Vass, W.C. and Beguinot, L. (1995) J. Biol. Chem. 270, 19557–19562.
[6] Webster, M.K. and Donoghue, D.J. (1996) EMBO J. 15, 520–527.
[7] Bargmann, C.I. and Weinberg, R.A. (1988) EMBO J. 7, 2043–2052.
[8] Stern, D.F. and Kamps, M.P. (1988) EMBO J. 7, 995–1001.
[9] Weiner, D.B., Liu, J., Cohen, J.A., Williams, W.V. and Greene, M.I. (1989) Nature 339, 230–231.
[10] Yarden, Y. and Ullrich, A. (1988) Annu. Rev. Biochem. 57, 443–478.
[11] Sternberg, M.J. and Gullick, W.J. (1990) Protein Eng. 3, 245–248.
[12] Smith, S.O., Smith, C.S. and Bormann, B.J. (1996) Nat. Struct. Biol. 3, 252–258.
[13] Burke, C.L. and Stern, D.F. (1998) Mol. Cell. Biol. 18, 5371–5379.
[14] Sajot, N. and Genest, M. (2001) J. Biomol. Struct. Dyn. 19, 15–31.
[15] Jones, D.H., Ball, E.H., Sharpe, S., Barber, K.R. and Grant, C.W. (2000) Biochemistry 39, 1870–1878.
[16] Sharpe, S., Barber, K.R. and Grant, C.W. (2002) Biochemistry 41, 2341–2352.
[17] Brandt-Rauf, P.W., Pincus, M.R. and Chen, J.M. (1989) J. Protein Chem. 8, 749–756.
[18] Brandt-Rauf, P.W., Rackovsky, S. and Pincus, M.R. (1990) Proc. Natl. Acad. Sci. USA 87, 8660–8664.
[19] Duneau, J.P., Garnier, N. and Genest, M. (1997) J. Biomol. Struct. Dyn. 15, 555–572.
[20] Gullick, W.J., Bottomley, A.C., Lofts, F.J., Doak, D.G., Mulvey, D., Newman, R., Crumpton, M.J., Sternberg, M.J. and Campbell, I.D. (1992) EMBO J. 11, 43–48.
[21] Goetz, M., Carlotti, C., Bontems, F. and Dufourc, E.J. (2001) Biochemistry 40, 6534–6540.
[22] Sajot, N. and Genest, M. (2000) Eur. Biophys. J. 28, 648–662.
[23] Shaka, A.J., Lee, C.J. and Pines, A. (1988) J. Magn. Reson. 77, 274–293.
[24] Piotto, M., Saudek, V. and Sklenar, V. (1992) J. Biomol. NMR 2, 661–665.
[25] Wüthrich, K., Billeter, M. and Braun, W. (1983) J. Mol. Biol. 169, 949–961.
[26] Brünger, A.T. (1987) X-PLOR Manual. Yale University, New Haven, CT.
[27] Nilges, M., Clore, G.M. and Gronenborn, A.M. (1988) FEBS Lett. 229, 317–324.
[28] Nilges, M., Kuszewski, J. and Brünger, A.T. (2002) Computational Aspects of the Study of Biological Macromolecules by NMR, Plenum Press, New York.
[29] Sambrook, J., Fritsch, E.F. and Maniatis, T. (1989) Molecular Cloning: A Laboratory Manual. Cold Spring Harbor Laboratory Press, Plainview, NY.
[30] Schägger, H. (1994) in: A Practical Guide to Membrane Protein Purification (Schägger, H. and Von Jagow, G., Eds.), Academic Press, San Diego, CA.
[31] Williamson, M.P. (1990) Biopolymers 29, 1423–1431.
[32] Grisshammer, R. and Tate, C.G. (1995) Q. Rev. Biophys. 28, 315–422.
[33] Gaffney, B.J. (1996) Annu. Rev. Biophys. Biomol. Struct. 25, 431–459.
[34] Keefe, L.J., Sondek, J., Shortle, D. and Lattman, E.E. (1993) Proc. Natl. Acad. Sci. USA 90, 3275–3279.
[35] Vainshtein, B.K., Melik-Adamyan, W.R., Barynin, V.V., Vagin, A.A., Grebenko, A.I., Borisov, V.V., Bartels, K.S., Fita, I. and Rossmann, M.G. (1986) J. Mol. Biol. 188, 49–61.
[36] Guntert, P., Mumenthaler, C. and Wüthrich, K. (1997) J. Mol. Biol. 273, 283–298.
[37] Mendrola, J.M., Berger, M.B., King, M.C. and Lemmon, M.A. (2002) J. Biol. Chem. 277, 4704–4712.
[38] Koradi, R., Billeter, M. and Wüthrich, K. (1996) J. Mol. Graph. 14, 21–32.